Agnieszka Jędrzejewska · Fragkoulis Kanavaris ·
Miguel Azenha · Farid Benboudjema ·
Dirk Schlicke
Editors

International RILEM Conference on Synergising Expertise towards Sustainability and Robustness of Cement-based Materials and Concrete Structures

SynerCrete'23 - Volume 2

Springer

Editors
Agnieszka Jędrzejewska
Department of Structural Engineering
Silesian University of Technology
Gliwice, Poland

Miguel Azenha
ISISE
University of Minho
Guimaraes, Portugal

Dirk Schlicke
Institute of Structural Concrete
Graz University of Technology
Graz, Austria

Fragkoulis Kanavaris
Technical Specialist Services, Materials
ARUP
London, UK

Farid Benboudjema
Laboratoire de Mécanique Paris-Saclay
ENS Paris-Saclay
Gif-sur-Yvette, France

ISSN 2211-0844 ISSN 2211-0852 (electronic)
RILEM Bookseries
ISBN 978-3-031-33186-2 ISBN 978-3-031-33187-9 (eBook)
https://doi.org/10.1007/978-3-031-33187-9

This Springer imprint is published by the registered company Springer Nature Switzerland AG
The registered company address is: Gewerbestrasse 11, 6330 Cham, Switzerland

Effect of Activator Solutions on the Thixotropic Behavior of Alkali-Activated Slag Concrete

Yubo Sun[1(✉)], Saeid Ghorbani[1], Guang Ye[1,2], and Geert De Schutter[1]

[1] Department of Structural Engineering and Building Materials, Magnel-Vandepitte Laboratory, Ghent University, 9052 Ghent, Belgium
Yubo.Sun@UGent.be

[2] Microlab, Section of Materials and Environment, Faculty of Civil Engineering and Geosciences, Delft University of Technology, Stevinweg 1, 2628 CN Delft, The Netherlands

Abstract. Alkali-activated material (AAM) is developed as a green alternative binder to replace Portland cement (PC) in the construction field. However, the large-scale application with AAM concrete is limited so far, with the insufficient knowledge of rheological behavior being a major obstruct.

Thixotropy of concrete is of great interest, which can be helpful to predict various early-age performances. The current study dedicates to evaluating the thixotropy of alkali-activated slag (AAS) concrete mixtures with different silicate and water content in activator solutions. In specific, the silicate modulus (Ms) and water to binder (w/b) ratio have been varied. The thixotropic index calculated by the initial and equilibrium shear stress from the stress growth test, as well as the breakdown area obtained by applying different shear speeds were used to evaluate the thixotropy of AAM concrete. Results indicate a good correlation between different approaches. It was found that an increase in Ms led to more pronounced thixotropic behaviors in AAS concrete due to the rapid nucleation and accumulation of early hydration products, resulting in significant increases in peak torque values and slight reductions of torque at equilibrium. Besides, the concrete thixotropy gradually declined by applying a higher w/b ratio.

Keywords: Alkali-activated slag · Activators · Concrete · Rheology · Thixotropy

1 Introduction

As a green alternative binding material to replace Portland cement (PC) in concrete constructions, alkali-activated materials (AAMs) have been extensively studied in recent years [1–3]. The application of AAMs not only reduces the greenhouse gases emission induced by PC clinker [4–7], but they could also provide promising mechanical properties [8–10] and even better chemical/fire resistance [10, 11] compared to PC materials. Despite the advantages, the underlying mechanism of rheology evolution in AAMs has been much less revealed in the literature and is not yet well understood. Rapid slump loss, high viscosity, and uncontrolled setting process have been frequently reported, especially in some alkali-activated slag (AAS) mixtures with a high dosage of silicate [12–14].

A. Jędrzejewska et al. (Eds.): SynerCrete 2023, RILEM Bookseries 44, pp. 325–336, 2023.
https://doi.org/10.1007/978-3-031-33187-9_31

In recent years, the thixotropic behavior of fresh cementitious materials has attracted more attention with the development of advanced concrete technologies [15–17]. Concrete thixotropy is of great importance, which is closely correlated to the early stiffening process upon extrusion or casting. The structural build-up of cement mixtures is ascribed to the colloidal flocculation between solid particles and the nucleation of reaction products at contact points [18]. Depending on the intensity of shear energy applied, the structuration could be partially recovered due to the breaking of interparticle linkages, whereas the dispersed particles are reconnected to each other through freshly formed hydration products as the reaction progress [15]. On the other hand, the local interparticle connections are continuously reinforced due to the accumulation of reaction products. Irreversible structuration could be developed in the case of a long resting period, as the mixing power becomes insufficient to break the rigid links between cement grains [15, 19].

Thixotropy has been widely investigated in PC materials. Starting from the origins, effects of various mix design parameters, supplementary cementitious materials, and admixtures have been well elaborated to interpret the thixotropic structural build-up and breakdown in fresh concrete mixtures [15, 16]. Moreover, it has been revealed that a proper understanding of the thixotropic behavior can be helpful to assess various time-dependent performances of concrete, such as the static stability [20], variation of the formwork pressure [21, 22], pumpability [23], interlayer quality during multilayer casting operations [24], and the construction rate of 3D printing applications [25, 26]. In AAMs, however, the thixotropic behavior has been only briefly assessed in several studies on pastes and mortars. Relevant research on the thixotropy of AAM concrete is very limited to date.

Therefore, the main objective of the current study is to further explore the thixotropic behavior of AAS concrete. The degree of thixotropy was assessed through different approaches, including the thixotropic index calculated from rheological parameters, as well as the breakdown area obtained with various shear speeds. Attempts have been made to correlate the thixotropy determined with different approaches. Results obtained may provide a better understanding of flow properties and thixotropic behavior, which would contribute to future practical applications with AAS concrete.

2 Materials and Methods

2.1 Materials

The ground granulated blast furnace slag (BFS) used in this study was provided by Ecocem Benelux B.V., with a density of 2890 kg/m^3. The particle size distribution measured by laser diffraction is given in Fig. 1(a), ($d_{50} = 8.28$ μm). Morphology of BFS particles was observed with a scanning electron microscope (SEM), as shown in Fig. 1(b). BFS particles have an irregular shape with high angularity. Details of the chemical composition of BFS determined by X-ray fluorescence (XRF) are listed in Table 1.

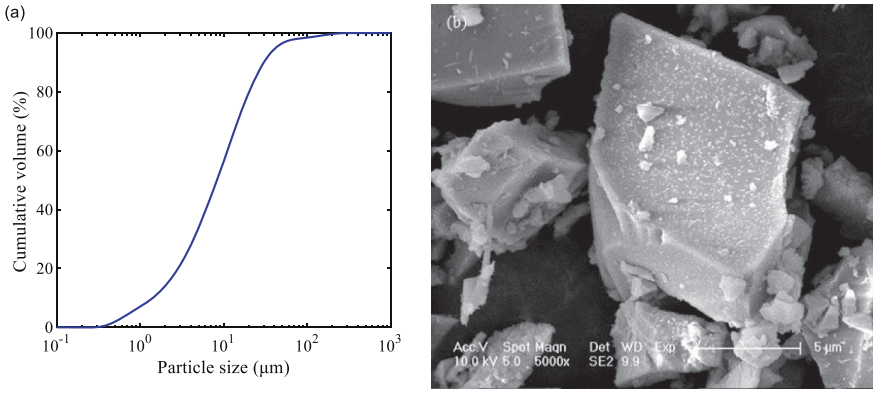

Fig. 1. Physical properties of BFS (a) Particle size distribution; (b) Morphology by SEM (5000 × magnification).

Table 1. Chemical composition of BFS measured by XRF (by mass %).

CaO	SiO_2	Al_2O_3	MgO	SO_3	TiO_2	K_2O	Fe_2O_3	MnO	ZrO_2	Other
40.90	31.10	13.70	9.16	2.31	1.26	0.69	0.40	0.31	0.12	0.05

Sodium hydroxide and sodium silicate were applied as activators in this study. Reagent-grade sodium hydroxide anhydrous pearls were provided by Brenntag N.V., and the sodium silicate solution (15% Na_2O, 30% SiO_2, and 55% water) was provided by PQ Corporation. River sand and gravel were used as fine and coarse aggregates to prepare AAS concrete, respectively. Their specific gravities and water absorption are presented in Table 2. Aggregates used in this study were air dried before mixing.

Table 2. Physical properties of aggregates.

Aggregate	Sand 0–4 mm	Coarse 2–8 mm	Coarse 8–16 mm
Specific gravity	2.65	2.64	2.67
Water absorption (%)	0.33	0.65	0.55

2.2 Mixture Proportions

Mixture proportions of AAS concrete are illustrated in Table 3. In total 9 mixtures were designed with a constant precursor content of 400 kg/m^3 to assess the effect of activator solutions on the properties of AAS concrete. The sodium concentration of activators (equivalent Na_2O content by the mass of precursor) was kept constant at 4% [27], while the w/b ratio ranged between 0.4 and 0.5 among AAS concretes to ensure adequate

consistency. Meanwhile, Ms was varied from 0.25 to 0.75 in different mixtures since higher values resulted in a very rapid setting in trial mixes. As presented in Table 3, M1 was designed with the lowest Ms (0.25) and w/b ratio (0.4) among all mixtures as the reference in this study. By modifying the composition of alkali activators, variations per unit volume of AAS concrete were compensated with the aggregate content. The aggregate packing of AAS concrete was designed to fall between A16 and B16 curves indicated in DIN 1045-2. An estimation was made that each AAS concrete mixture contains 1% air content [28]. Activator solutions were prepared by dissolving the alkaline compounds in tap water 24 h before mixing.

Table 3. Mixture proportions of AAS concretes.

Mix	BFS (kg/m^3)	Activator				w/b[b]	Aggregate (kg/m^3) [c]		
		Sodium hydroxide (kg/m^3)	Sodium silicate (kg/m^3)	Ms [a]	Extra water (kg/m^3)		0–4 mm	2–8 mm	8–16 mm
M1	400	18.06	13.33	0.25	162.29	0.4	715	491	583
M2	400	18.06	13.33		183.50	0.45	692	476	565
M3	400	18.06	13.33		204.70	0.5	670	460	547
M4	400	15.48	26.67	0.5	156.33	0.4	712	490	581
M5	400	15.48	26.67		177.70	0.45	689	474	563
M6	400	15.48	26.67		199.08	0.5	667	458	544
M7	400	12.90	40.00	0.75	150.36	0.4	709	488	579
M8	400	12.90	40.00		171.91	0.45	686	472	560
M9	400	12.90	40.00		193.45	0.5	664	456	542

[a]Defined as the molar ratio between SiO_2 and Na_2O in the activator
[b]Defined as water content in both aqueous activator and extra water added separately divided by the sum of precursor and solid activators
[c]Designed to reach between A16 and B16 curves indicated in DIN 1045–2

2.3 Testing Program

AAS concrete was prepared in 20 L batches by following the same mixing protocol. The solid components including BFS and aggregates were first dry-blended in a planetary mixer for 2 min. Afterwards, the activator solution was added to the mixer (in 30 s) and mixed for another 3 min to derive the fresh AAS concrete for subsequent tests. Rheological tests were conducted using an ICAR Plus rheometer with the fresh AAS concrete to determine the rheological parameters. As shown in Fig. 2, the rheometer has a coaxial cylinder geometry fitted with a 4-blade vane, and ribs are attached to the container wall to prevent slippage. In this study, due to the strong early reactivities of AAS mixtures [29], the thixotropic build-up was evaluated on 5 min basis through different approaches.

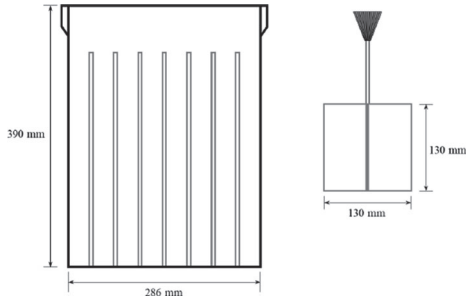

Fig. 2. Geometry of the ICAR Plus rheometer.

In the first method, the thixotropic index of AAS concrete was calculated from the peak and equilibrium shear stresses along the stress growth test with a constant rotational speed of 0.025 rps for 60 s [30]. Fresh concrete was first remixed for 1 min and left at rest for 5 min until the stress growth test. A typical profile is shown in Fig. 3, it can be seen that the torque first reached a maximum value after the initial steep increase, which indicates the majority of particle interactions were broken down, allowing the flow of AAS concrete. After yielding, the torque progressively declined until an equilibrium state, reflecting the energy required to maintain a steady flow. The peak shear stress τ_0 was determined from the maximum torque observed, whereas the equilibrium shear stress τ_e was obtained through the average torque of the last 10 s. Torque values were converted into shear stresses with Eq. (1) [31], and the thixotropic index was expressed as $[(\tau_0\text{-}\tau_e)/\tau_e]$ [21].

$$\tau_0 = \frac{2T_m}{\pi D^3(\frac{h}{D} + \frac{1}{3})} \tag{1}$$

where:
τ_0 is the static yield stress in Pa,
T_m is the maximum torque in Nm,
D is the diameter of the vane in m,
h is the height of the vane in m.

Moreover, the breakdown area with different rotational speeds was calculated to assess the thixotropic behavior [32, 33]. AAS concrete was remixed for 1 min and rested for another 5 min, followed by the shear step with a fixed rotational speed of 0.15 rps for 30 s until an equilibrium state. Subsequently, the 5-min rest and shear procedures were repeated with higher speeds of 0.3, 0.45, and 0.6 rps. At each speed, the initial peak torque was recorded as T_0, whereas the average value of the last 10 s was determined as the torque at equilibrium (T_e). Accordingly, as shown in Fig. 4, the thixotropic behavior of AAS concrete could be quantified by the breakdown area between the initial and equilibrium torque curves.

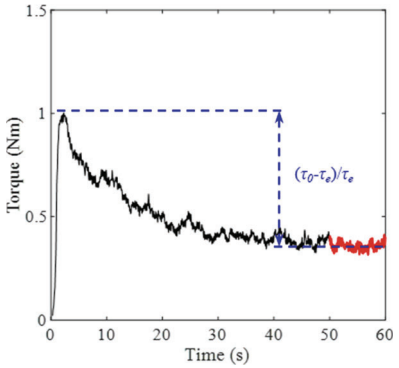

Fig. 3. Typical curve of the torque evolution obtained from a stress growth test (represented with M9).

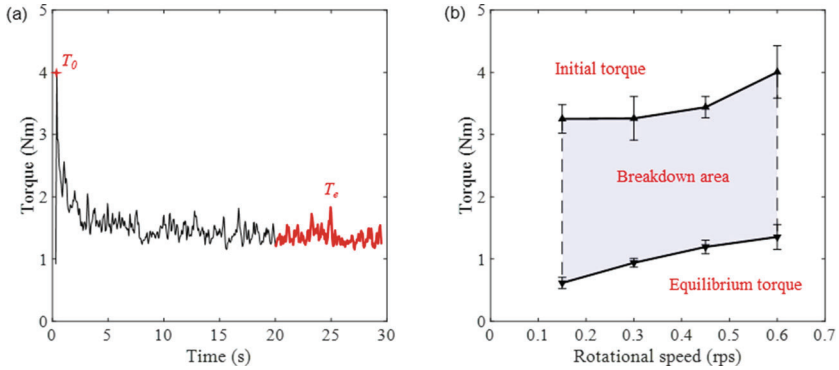

Fig. 4. Typical calculation of the breakdown area (represented with M9) (a) Torque evolution as a function of time at N = 0.6 rps; (b) Breakdown area between the initial and equilibrium torque curves.

3 Results and Discussions

The thixotropic performance of AAS concrete was first assessed by the stress growth test given a 5-min resting duration. As presented in Fig. 5, the degree of thixotropy was reflected by the thixotropic index calculated by $[(\tau_0-\tau_e)/\tau_e]$. The maximum degree of thixotropy was detected in M7 (Ms0.75, w/b = 0.4) among all AAS concretes, which is about 3 times higher than that of M1 (Ms0.25, w/b = 0.4). It was found that the thixotropic behavior of AAS concrete was significantly enhanced with an increase in Ms. On the other hand, the water content showed a negative impact on the thixotropic behavior of AAS concrete. Comparing to M7, the thixotropic index reduced by 68% and 89% for M8 and M9 with higher w/b ratios, respectively.

Besides, fresh AAS concrete was also tested with constant rotational speeds of 0.15, 0.3, 0.45, and 0.6 rps with the same 5-min rest period. As illustrated in Table 4, the AAS concrete thixotropy was evaluated with the breakdown area between initial and equilibrium torque values (T_0 and T_e).

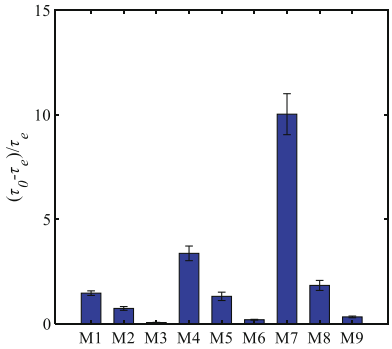

Fig. 5. Thixotropic index of AAS concretes.

Table 4. Torque values and the breakdown area of AAS concretes.

	T_0 (Nm) a				T_e (Nm) b				Breakdown area ($J/m^3 \cdot s$)
	0.15 rps	0.3 rps	0.45 rps	0.6 rps	0.15 rps	0.3 rps	0.45 rps	0.6 rps	
M1	12.63	15.99	19.64	20.31	6.04	8.23	9.77	10.28	1011.52
M2	3.59	4.36	5.45	6.50	2.32	3.15	3.94	4.27	156.31
M3	1.41	1.86	2.04	2.08	0.64	1.03	1.23	1.47	81.30
M4	20.23	20.58	21.44	23.26	6.04	7.80	8.93	9.76	1368.45
M5	4.32	7.80	8.67	9.66	1.76	2.31	2.97	3.27	547.68
M6	1.42	2.11	2.33	2.54	0.61	0.94	1.19	1.36	115.54
M7	28.01	29.23	30.92	31.75	5.35	7.40	8.61	9.32	2331.98
M8	6.20	9.03	10.20	10.59	1.33	2.03	2.49	2.89	734.46
M9	3.25	3.26	3.44	4.00	0.60	0.89	1.08	1.26	259.54

[a]Initial torque values
[b]Equilibrium torque values

The incorporation of higher silicate content in the activator improved the thixotropy through a significant increase in T_0, accompanied with slight reductions of T_e in corresponding mixtures. Among all AAS concretes, the greatest T_0 was detected in M7 (Ms0.75, w/b = 0.4) at 0.6 rps, which was much higher than that of M1 and M4 under the same rotational speed. It is indicated a stronger shear energy is required to break down the interparticle interactions and initiate the flow. On the other hand, M7 exhibited lower T_e than M1 and M4, suggesting less shear energy is required to maintain a steady flow. Similar results have been observed in other mixtures with higher w/b ratios. By contrast, both T_0 and T_e significantly declined with an increase in the w/b ratio, leading to less thixotropic behavior of AAS concrete. It can be inferred that the alkalinity of the pore solution was reduced since the activator was diluted with the extra water content, which slowed down the dissolution of slag particles. Meanwhile, porous microstructures with

bigger interstitial voids were formed with a higher w/b ratio. In that case, more reaction products are required to contribute to the interactions between slag particles, thereby less thixotropic behavior was observed.

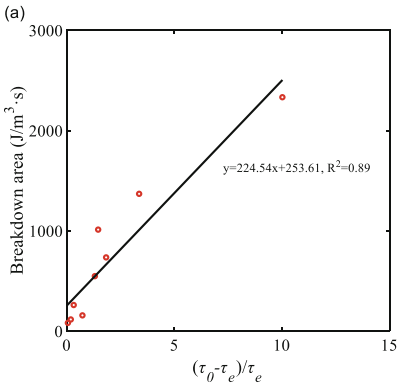

Fig. 6. Relationship between the AAS concrete thixotropic parameters.

Furthermore, relationships among results obtained through different approaches are plotted in Fig. 6. Good correlations have been observed with an R^2 of about 0.9. It is indicated that either approach might provide a reliable estimation of the degree of thixotropy in AAS concrete.

In PC materials, it has been suggested that the thixotropy originates from the colloidal flocculation and interparticle connections (through early hydration products bridges such as C-S-H and ettringite) between cement particles [18, 33]. However, it was reported that the silicate in the activator presents as interstitial gels to disperse the slag grains in AAS [34], whereas silicate-activated AAMs exhibit negligible colloidal interactions between precursor particles due to the strong viscous effect [14, 35]. From the initial microstructural configuration point of view, it appears that the silicate content in the activator plays a negative role in the thixotropic behavior of AAS concrete, which is in contradiction to the result illustrated in Fig. 5.

Nevertheless, the thixotropic behavior in cementitious materials is also dependent on the chemical reaction progress during the rest period. Considering the activation reaction, previous studies have revealed the seeding effect of silicate species in the activator, which may promote the nucleation of reaction products in the pore solution [36, 37]. Palacios et al. [29] further revealed the high early reactivity and rapid accumulation of early reaction products in high-Ms AAS mixtures. As a consequence, the volume fraction and surface area are significantly improved in the system, leading to increases in the number of interparticle connections and the level of attractive forces between solid particles [33]. It can be analogized to the effect of set-accelerating admixtures in PC materials, where the thixotropic behavior is enhanced due to the formation of numerous fine particles [32]. Accordingly, higher initial torque is required to break down the flocculation between solid particles and initiate the flow of high-Ms AAS concrete. On the other hand, the reduction of torque at equilibrium with the increase of

Ms could be attributed to that flocculated structures and early reaction products formed are progressively broken down into smaller particles, which might fill the interstitial voids and provide additional lubricant around solid grains [33, 38]. Further, the extra silicate content from the activator may disperse the slag particles, leading to a fluidizing effect under dynamic flow conditions [34, 39]. Therefore, lower shear energy is required to maintain the steady-state flow. Thereby, the thixotropic behavior of AAS concrete became more explicit with an increase in Ms.

Apart from that, previous studies have reported that activators with a lower Ms contain more monomers and dimers, whereas larger oligomers and polymeric species become predominant with the increase of Ms [40, 41]. It is indicated that long-chain polymer structures may contribute to stronger cohesiveness in the mixture at rest due to entanglements and associations [32]. However, such effect is terminated once the flow is initiated, since their spatial distributions become parallel to the flow direction. Thereby, the thixotropy of AAS mixtures could be also correlated to the inherent property of activator solutions.

In a word, distinct structural build-up behaviors of AAS concretes have been observed at early ages in this study by varying Ms in activators. The structuration is ascribed to the flocculation and early onset of chemical reactions during the acceleration stage, where the latter could hardly be broken down by remixing. AAS concrete with higher Ms exhibited stronger thixotropic build-up, which can be partially recovered through the remixing process. It is noticed that the thixotropic build-up in high-Ms mixtures was developed at early ages before acceleration stage reactions, which is attributed to the strong early reactivity [29]. High-Ms AAS concrete in turn may exhibit good workability retention after eliminating the thixotropic behavior. Similarly, it has been proposed that the fluidity of silicate-activated AAS mixtures could be maintained by extending the mixing time [30, 42].

4 Conclusions

This research aims to provide an assessment on the thixotropic behavior of alkali-activated slag (AAS) concretes by varying the silicate modulus (Ms) and water to binder (w/b) ratios. Thixotropy of AAS concrete was assessed through different approaches, including the thixotropic index calculated from the peak and equilibrium shear stresses in stress growth test, as well as the breakdown area under different rotational speeds. Good correlations were found between different methods, thus the AAS concrete thixotropy could be evaluated by either approach. It was found that the increase in Ms resulted in more pronounced thixotropic behavior of AAS concrete, accompanied with significant increases in peak torque values and slight reductions of torque at equilibrium. Meanwhile, the concrete thixotropy gradually declined by increasing the w/b ratio.

Appendix

(See Fig. 7).

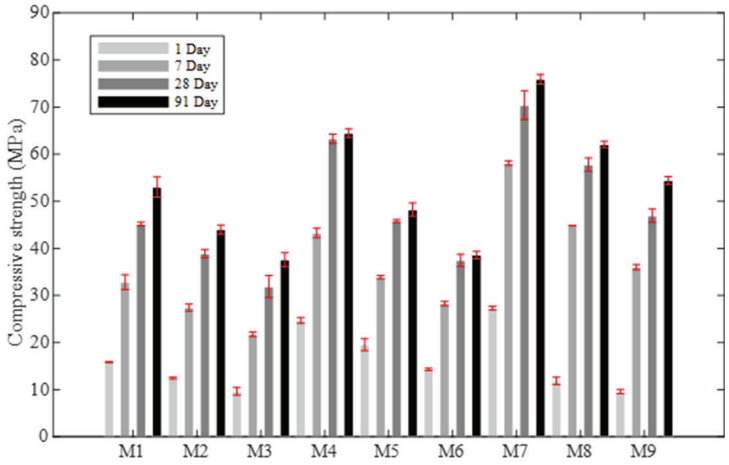

Fig. 7. Compressive strength development of AAS concretes.

References

1. van Deventer, J.S.J., Provis, J.L., Duxson, P., Brice, D.G.: Chemical research and climate change as drivers in the commercial adoption of alkali activated materials. Waste Biomass Valorizat. **1**(1), 145–155 (2010). https://doi.org/10.1007/s12649-010-9015-9
2. Provis, J.L., Deventer, J.S.J. (eds.): Alkali activated materials. RSR, vol. 13. Springer, Dordrecht (2014). https://doi.org/10.1007/978-94-007-7672-2
3. Turner, L.K., Collins, F.G.: Carbon dioxide equivalent (CO2-e) emissions: a comparison between geopolymer and OPC cement concrete. Constr. Build. Mater. **43**, 125–130 (2013)
4. Mehta, K.P.: Reducing the environmental impact of concrete. Concr. Int. **23**, 61–66 (2001)
5. Huntzinger, D.N., Eatmon, T.D.: A life-cycle assessment of Portland cement manufacturing: comparing the traditional process with alternative technologies. J. Clean. Prod. **17**, 668–675 (2009)
6. Chen, C., Habert, G., Bouzidi, Y., Jullien, A.: Environmental impact of cement production: detail of the different processes and cement plant variability evaluation. J. Clean. Prod. **18**, 478–485 (2010)
7. Scrivener, K.L.: Options for the future of cement. Indian Concr. J. **88**, 11–21 (2014)
8. Fernández-Jiménez, A., Palomo, J.G., Puertas, F.: Alkali-activated slag mortars: mechanical strength behaviour. Cem. Concr. Res. **29**, 1313–1321 (1999). https://doi.org/10.1016/S0008-8846(99)00154-4
9. Luukkonen, T., Abdollahnejad, Z., Yliniemi, J., Kinnunen, P., Illikainen, M.: One-part alkali-activated materials: a review. Cem. Concr. Res. **103**, 21–34 (2018). https://doi.org/10.1016/j.cemconres.2017.10.001
10. Provis, J.L.: Geopolymers and other alkali activated materials: why, how, and what? Mater. Struct. **47**(1–2), 11–25 (2013). https://doi.org/10.1617/s11527-013-0211-5
11. Aiken, T.A., Sha, W., Kwasny, J., Soutsos, M.N.: Resistance of geopolymer and Portland cement based systems to silage effluent attack. Cem. Concr. Res. **92**, 56–65 (2017). https://doi.org/10.1016/j.cemconres.2016.11.015
12. Palacios, M., Banfill, P.F.G., Puertas, F.: Rheology and setting of alkali-activated slag pastes and mortars: effect of organic admixture. ACI Mater. J. **105**, 140 (2008)
13. Jansson, H., Bernin, D., Ramser, K.: Silicate species of water glass and insights for alkali-activated green cement. AIP Adv. **5**, 06716 (2015). https://doi.org/10.1063/1.4923371

14. Alnahhal, M.F., Kim, T., Hajimohammadi, A.: Distinctive rheological and temporal viscoelastic behaviour of alkali-activated fly ash/slag pastes: a comparative study with cement paste. Cem. Concr. Res. **144**, 106441 (2021). https://doi.org/10.1016/j.cemconres.2021.106441
15. Jiao, D., De Schryver, R., Shi, C., De Schutter, G.: Thixotropic structural build-up of cement-based materials: a state-of-the-art review. Cem. Concr. Compos. **122**, 104152 (2021)
16. Wallevik, J.E.: Rheological properties of cement paste: thixotropic behavior and structural breakdown. Cem. Concr. Res. **39**, 14–29 (2009). https://doi.org/10.1016/j.cemconres.2008.10.001
17. Jiao, D., Shi, C., Yuan, Q., An, X., Liu, Y., Li, H.: Effect of constituents on rheological properties of fresh concrete-a review. Cem. Concr. Compos. **83**, 146–159 (2017). https://doi.org/10.1016/j.cemconcomp.2017.07.016
18. Roussel, N., Ovarlez, G., Garrault, S., Brumaud, C.: The origins of thixotropy of fresh cement pastes. Cem. Concr. Res. **42**, 148–157 (2012). https://doi.org/10.1016/j.cemconres.2011.09.004
19. Wallevik, J.E.: Thixotropic investigation on cement paste: experimental and numerical approach. J. Nonnewton. Fluid Mech. **132**, 86–99 (2005)
20. Khayat, K.H.,x Saric-Coric, K.H., Liotta, F.: Influence of thixotropy on stability characteristics of cement grout and concrete. ACI Mater. J. **99**, 234–241 (2002). https://doi.org/10.14359/11968
21. Assaad, J., Khayat, K.H., Mesbah, H.: Variation of formwork pressure with thixotropy of self-consolidating concrete variation of formwork pressure with thixotropy of self-consolidating concrete (2003)
22. Assaad, J., Khayat, K.H.: Assessment of thixotropy of self-consolidating concrete and concrete-equivalent-mortar-effect of binder composition and content. ACI Mater. J. **101**(5), 400–408 (2004)
23. Feys, D., Verhoeven, R., De Schutter, G.: Influence of thixotropy on pressures required during pumping of concrete. In: AIP Conference Proceedings, pp. pp. 710–712. American Institute of Physics (2008)
24. Roussel, N., Cussigh, F.: Distinct-layer casting of SCC: the mechanical consequences of thixotropy. Cem. Concr. Res. **38**, 624–632 (2008)
25. Reiter, L., Wangler, T., Roussel, N., Flatt, R.J.: The role of early age structural build-up in digital fabrication with concrete. Cem. Concr. Res. **112**, 86–95 (2018)
26. Mechtcherine, V., et al.: Extrusion-based additive manufacturing with cement-based materials–production steps, processes, and their underlying physics: a review. Cem. Concr. Res. **132**, 106037 (2020)
27. Zhang, S., Li, Z., Ghiassi, B., Yin, S., Ye, G.: Fracture properties and microstructure formation of hardened alkali-activated slag/fly ash pastes. Cem. Concr. Res. **144**, 106447 (2021)
28. Provis, J.L., et al.: RILEM TC 247-DTA round robin test: mix design and reproducibility of compressive strength of alkali-activated concretes. Mater. Struct. **52**(5), 1–13 (2019). https://doi.org/10.1617/s11527-019-1396-z
29. Palacios, M., et al.: Early reactivity of sodium silicate-activated slag pastes and its impact on rheological properties. Cem. Concr. Res. **140**, 106302 (2021). https://doi.org/10.1016/j.cemconres.2020.106302
30. Puertas, F., et al.: Alkali-activated slag concrete: fresh and hardened behaviour. Cem. Concr. Compos. **85**, 22–31 (2018). https://doi.org/10.1016/j.cemconcomp.2017.10.003
31. Koehler, E.P., Fowler, D.W.: Development of a portable rheometer for fresh portland cement concrete (2004)
32. Assaad, J., Khayat, K.H., Mesbah, H.: Assessment of thixotropy of flowable and self-consolidating concrete, ACI Mater. J. **100**, 99–107 (2003). https://doi.org/10.14359/12548

33. Ahari, R.S., Erdem, T.K., Ramyar, K.: Thixotropy and structural breakdown properties of self consolidating concrete containing various supplementary cementitious materials. Cem. Concr. Compos. **59**, 26–37 (2015). https://doi.org/10.1016/j.cemconcomp.2015.03.009
34. Sun, Y., et al.: Rheology of alkali-activated slag pastes: new insight from microstructural investigations by cryo-SEM. Cem. Concr. Res. **157**, 106806 (2022). https://doi.org/10.1016/j.cemconres.2022.106806
35. Favier, A., Hot, J., Habert, G., Roussel, N., D'Espinose De Lacaillerie, J.B.: Flow properties of MK-based geopolymer pastes: a comparative study with standard Portland cement pastes. Soft Matter. **10**, 1134–1141 (2014). https://doi.org/10.1039/c3sm51889b
36. Hubler, M.H., Thomas, J.J., Jennings, H.M.: Influence of nucleation seeding on the hydration kinetics and compressive strength of alkali activated slag paste. Cem. Concr. Res. **41**, 842–846 (2011). https://doi.org/10.1016/j.cemconres.2011.04.002
37. Gebregziabiher, B.S., Thomas, R., Peethamparan, S.: Very early-age reaction kinetics and microstructural development in alkali-activated slag. Cem. Concr. Compos. **55**, 91–102 (2015). https://doi.org/10.1016/j.cemconcomp.2014.09.001
38. Tattersall, G.H., Banfill, P.F.G.: The rheology of fresh concrete (1983)
39. Alonso, M.M., Gismera, S., Blanco, M.T., Lanzón, M., Puertas, F.: Alkali-activated mortars: workability and rheological behaviour. Constr. Build. Mater. **145**, 576–587 (2017). https://doi.org/10.1016/j.conbuildmat.2017.04.020
40. Duxson, P., Provis, J.L., Lukey, G.C., Mallicoat, S.W., Kriven, W.M., Van Deventer, J.S.J.: Understanding the relationship between geopolymer composition, microstructure and mechanical properties. Colloids Surf. A Physicochem. Eng. Asp. **269**, 47–58 (2005). https://doi.org/10.1016/j.colsurfa.2005.06.060
41. Svensson, I.L., Sjöberg, S., Öhman, L.-O.: Polysilicate equilibria in concentrated sodium silicate solutions. J. Chem. Soc. Faraday Trans. 1 Phys. Chem. Condens. Phases. **82**, 3635–3646 (1986)
42. Puertas, F., Varga, C., Alonso, M.M.: Rheology of alkali-activated slag pastes: effect of the nature and concentration of the activating solution. Cem. Concr. Compos. **53**, 279–288 (2014). https://doi.org/10.1016/j.cemconcomp.2014.07.012